# Hadron Production Generators: Progress

Rakitha S. Beminiwattha

Department of Physics, Syracuse University

January $12^{\mathrm{th}}$, 2016

# Outline

# Issues with Wiser Generator

- The kinematics regions compatible with the wiser fit do not include all the phase-space of SoLID acceptance.
- The validity of the Wiser fit is checked using different data set obtained from SLAC and published in the reference [1] (Boyarski et. al.)

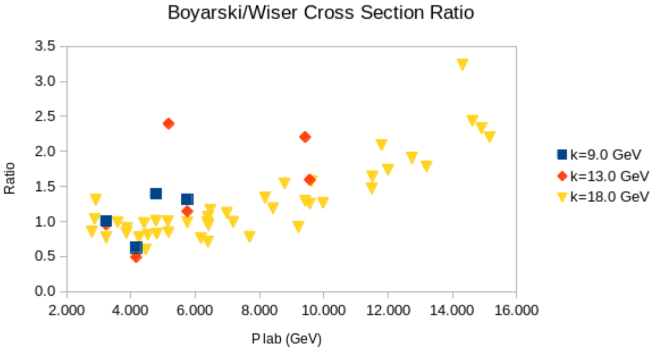


Figure: Cross section ratio for all transverse momentum

# Hall D Photo-Production Generator

- Hall D generator uses fits to various experimental data and SAID partial-wave analysis fits to generate photo-production cross sections for photon energies below $3\ \mathrm{GeV}$
- It uses modified version of PYTHIA for photon energies above $3\ \mathrm{GeV}$
  - Hall D generator support from Eugene Chudekov and Mark Ito

Following $\gamma + p^{+}$ reactions considered for photon energies below $11\ \mathrm{GeV}$

| Process | Fraction of Events | Energy Range |
|---|---|---|
| PYTHIA | 13 | $3.00 < E < 10.00\ GeV$ |
| $p^{+} + \pi^{0}$ | 25 | $0.15 < E < 3.00\ GeV$ |
| $n + \pi^{+}$ | 33 | |
| $p^{+} + \pi^{+} + \pi^{-} (non - res.)$ | 4 | |
| $p^{+} + \rho^{0}$ | 3 | |
| $\Delta^{++} + \pi^{-}$ | 7 | |
| $p^{+} + \pi^{0} + \pi^{0}$ | 2 | |
| $n + \pi^{+} + \pi^{0}$ | 9 | |
| $p^{+} + \eta^{0}$ | 1 | |
| $p^{+} + \pi^{+} + \pi^{-} + \pi^{0}$ | 3 | |
| $n + \pi^{+} + \pi^{+} + \pi^{-}$ | 1 | |

# Electro-Production with Hall-D Generator

- Photon energy is sampled using electro-production cross section weighted distribution
  - Where the total cross section is the sum of real (Bremsstrahlung) and virtual (EPA) contributions
- $11\ \mathrm{GeV}$ electron beam ($50\ \mu\mathrm{A}$) is incident into a $40\ \mathrm{cm}$ hydrogen target

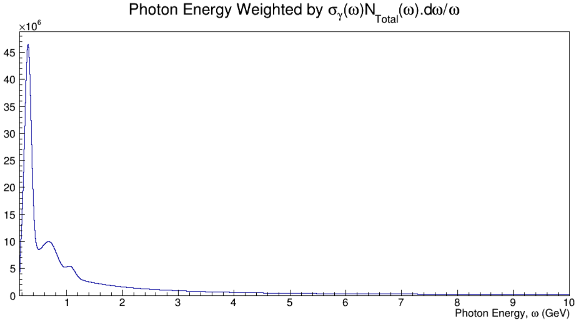


Figure: Hall D generator now samples the photon energy using electro-production cross section weighted distribution

# Cross Sections from Proton Target

Table: Using Geant4

| | $\pi^0$ | | $\pi^-$ | | $\pi^+$ | |
|---|---|---|---|---|---|---|
| Mom. Range (GeV) | xs (mb) | Rate (MHz) | xs (mb) | Rate (MHz) | xs (mb) | Rate (MHz) |
| 0 - 1 | 27.92 | 14922.27 | 12.39 | 6621.69 | 35.18 | 18801.05 |
| 1 - 2 | 3.25 | 1735.00 | 2.22 | 1185.79 | 2.70 | 1441.67 |
| 2 - 3 | 1.13 | 602.26 | 0.79 | 421.27 | 0.71 | 380.70 |
| 3 - 4 | 0.53 | 280.84 | 0.36 | 190.35 | 0.30 | 159.15 |
| 4 - 5 | 0.34 | 180.99 | 0.16 | 87.37 | 0.12 | 65.53 |
| 5 - 10 | 0.32 | 171.63 | 0.14 | 74.89 | 0.12 | 62.41 |
| Total | 33.48 | 17892.99 | 16.06 | 8581.36 | 39.13 | 20910.51 |

Table: Using Hall D Generator

| | $\pi^0$ | | $\pi^-$ | | $\pi^+$ | |
|---|---|---|---|---|---|---|
| Mom. Range (GeV) | xs (mb) | Rate (MHz) | xs (mb) | Rate (MHz) | xs (mb) | Rate (MHz) |
| 0 - 1 | 23.45 | 12532.33 | 11.50 | 6145.88 | 33.47 | 17888.18 |
| 1 - 2 | 2.18 | 1164.50 | 2.36 | 1258.96 | 3.10 | 1654.65 |
| 2 - 3 | 0.64 | 341.37 | 0.81 | 432.42 | 0.87 | 466.53 |
| 3 - 4 | 0.24 | 127.00 | 0.36 | 192.33 | 0.35 | 186.56 |
| 4 - 5 | 0.10 | 54.58 | 0.17 | 90.26 | 0.17 | 92.10 |
| 5 - 10 | 0.07 | 37.26 | 0.15 | 81.08 | 0.15 | 80.82 |
| Total | 26.68 | 14257.04 | 15.35 | 8200.93 | 38.11 | 20368.84 |

- G4 $\sigma(p)$ for $\pi^0$ is about 30% larger

# Pion Distribution from Proton Target

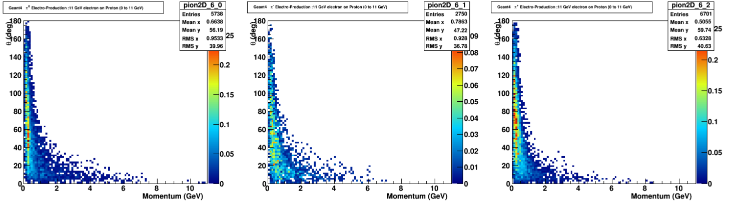


Figure: Using GEANT4

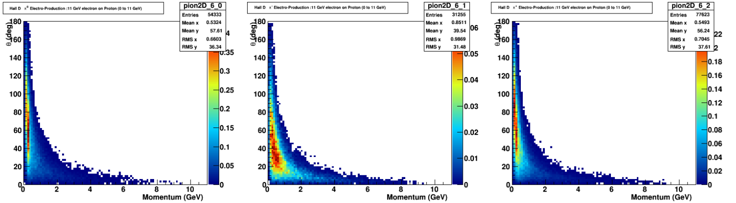


Figure: Using Hall D

# Deuterium Target using Hall D Generator

- Hall D generator only has proton cross section information
- Assumed isospin symmetry and used proton target events generated by hall D generator
  - Isospin symmetric deuterium cross sections using proton pion cross sections

$$\sigma(A)_{\pi^0} = Z \cdot \sigma_{\pi^0} + N \cdot \sigma_{\pi^0}$$
$$\sigma(A)_{\pi^\pm} = Z \cdot \sigma_{\pi^\pm} + N \cdot \sigma_{\pi^\pm}$$

In Wiser generator, $\sigma_{\pi^0} = \frac{\sigma_{\pi^+} + \sigma_{\pi^-}}{2}$

Table: Total Deuterium xs for $\theta < 90^o$ *deg*

| Pion Type | Wiser xs (mb) | Hall D xs (mb) | Geant4 xs (mb) | Hall D vs. G4 agreement (%) |
|---|---|---|---|---|
| $\pi^0$ | 189.7 | 43.0 | 84.8 | -97 |
| $\pi^-$ | 191.6 | 44.9 | 39.5 | 12 |
| $\pi^+$ | 192.7 | 44.9 | 38.7 | 14 |

# Cross Sections from Deuterium Target

Table: Using Geant4

| | $\pi^0$ | | $\pi^-$ | | $\pi^+$ | |
|---|---|---|---|---|---|---|
| Mom. Range | xs | Rate | xs | Rate | xs | Rate |
| (GeV) | (mb) | (MHz) | (mb) | (MHz) | (mb) | (MHz) |
| 0 - 1 | 79.40 | 50501.13 | 35.40 | 22514.30 | 36.15 | 22994.82 |
| 1 - 2 | 6.87 | 4371.82 | 5.81 | 3694.67 | 5.20 | 3304.61 |
| 2 - 3 | 2.25 | 1429.19 | 1.67 | 1064.09 | 1.31 | 833.17 |
| 3 - 4 | 1.21 | 770.76 | 0.77 | 489.92 | 0.53 | 333.89 |
| 4 - 5 | 0.65 | 411.91 | 0.34 | 218.44 | 0.28 | 174.75 |
| 5 - 10 | 0.97 | 614.74 | 0.34 | 215.31 | 0.25 | 159.15 |
| Total | 91.34 | 58099.55 | 44.33 | 28196.73 | 43.71 | 27800.39 |

Table: Using Hall D Generator

| | $\pi^0$ | | $\pi^-$ | | $\pi^+$ | |
|---|---|---|---|---|---|---|
| Mom. Range | xs | Rate | xs | Rate | xs | Rate |
| (GeV) | (mb) | (MHz) | (mb) | (MHz) | (mb) | (MHz) |
| 0 - 1 | 46.90 | 29830.49 | 44.97 | 28605.28 | 44.97 | 28605.28 |
| 1 - 2 | 4.36 | 2771.83 | 5.45 | 3467.62 | 5.45 | 3467.62 |
| 2 - 3 | 1.28 | 812.56 | 1.68 | 1069.88 | 1.68 | 1069.88 |
| 3 - 4 | 0.48 | 302.29 | 0.71 | 450.94 | 0.71 | 450.94 |
| 4 - 5 | 0.20 | 129.91 | 0.34 | 217.04 | 0.34 | 217.04 |
| 5 - 10 | 0.14 | 88.69 | 0.30 | 192.68 | 0.30 | 192.68 |
| Total | 53.35 | 33936.44 | 53.46 | 34003.77 | 53.46 | 34003.77 |

- From G4: $\sigma(D)$ for $\pi^0$ is about 34% larger wrt isospin symmetric $\sigma(2p)$
- From G4: $\sigma(D)$ for $\pi^\pm$ is about 25% smaller wrt isospin symmetric $\sigma(2p)$

# Pion Distribution from Deuterium Target

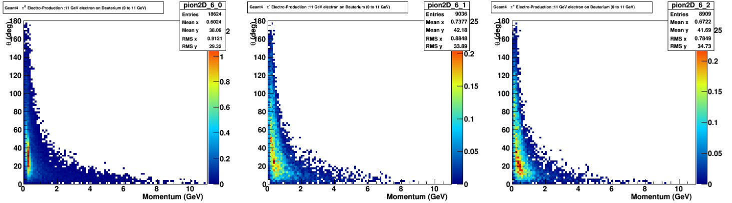


Figure: Using GEANT4

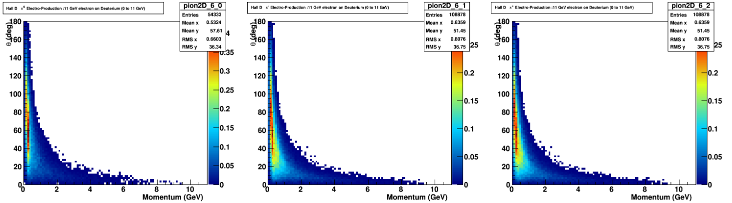


Figure: Using Hall D

# Pion Angular Distribution from Deuterium Target

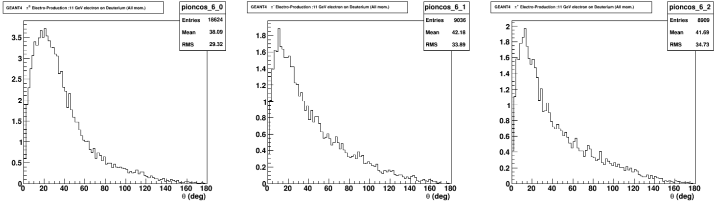


Figure: Using GEANT4

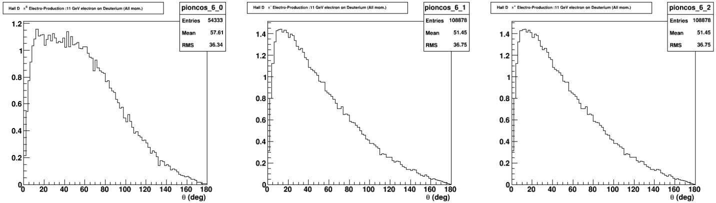


Figure: Using Hall D

# Cross Sections from Deuterium Target

| | Hall D $\pi^0$ | | Geant4 $\pi^0$ | |
|---|---|---|---|---|
| Mom. Range (GeV) | xs (mb) | Rate (MHz) | xs (mb) | Rate (MHz) |
| 0.0 - 0.1 | 1.10 | 700.76 | 3.56 | 2262.36 |
| 0.1 - 0.2 | 10.57 | 6726.01 | 15.40 | 9792.09 |
| 0.2 - 0.3 | 15.22 | 9680.26 | 25.28 | 16079.91 |
| 0.3 - 0.4 | 7.18 | 4565.59 | 14.22 | 9046.30 |
| 0.4 - 0.5 | 4.05 | 2576.95 | 7.44 | 4730.68 |
| 0.5 - 0.6 | 2.85 | 1813.12 | 4.47 | 2845.90 |
| 0.6 - 0.7 | 2.00 | 1274.74 | 3.09 | 1965.92 |
| 0.7 - 0.8 | 1.63 | 1033.66 | 2.48 | 1578.97 |
| 0.8 - 0.9 | 1.22 | 773.22 | 1.91 | 1213.87 |
| 0.9 - 1.0 | 1.08 | 685.15 | 1.55 | 986.08 |

# $\pi^0$ Distribution from Deuterium Target for $P < 1$ $GeV$

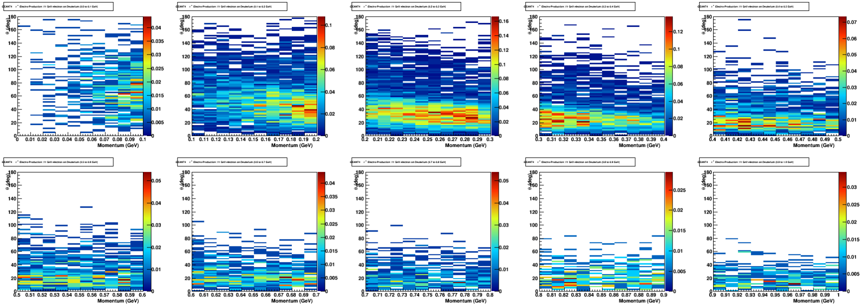


Figure: Using GEANT4

# $\pi^0$ Distribution from Deuterium Target for $P < 1\ GeV$

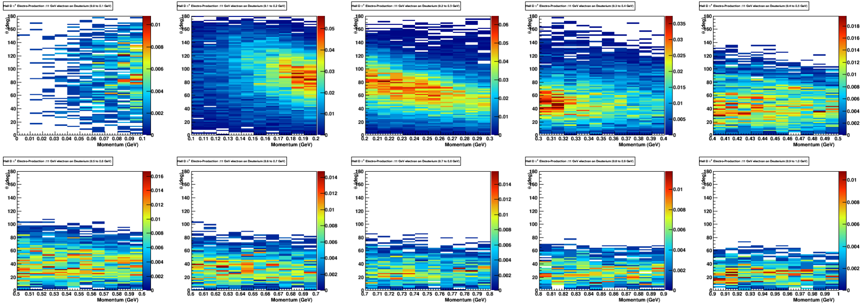

Figure: Using Hall D

# $\pi^0$ Angular Distribution from Deuterium Target for $P < 1\ GeV$

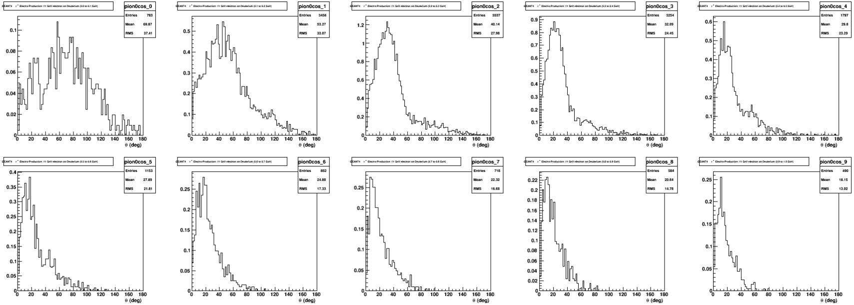


Figure: Using GEANT4

# $\pi^0$ Angular Distribution from Deuterium Target for $P < 1\ GeV$

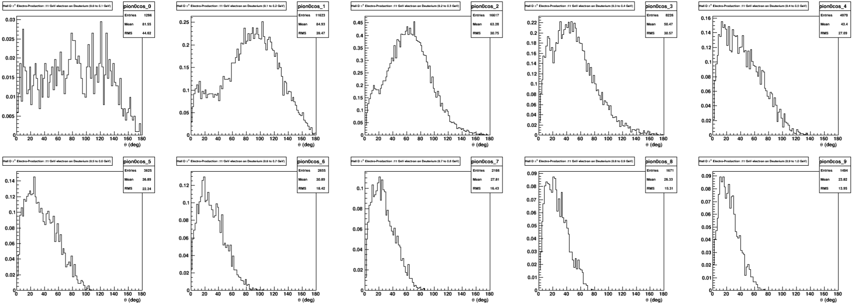


Figure: Using Hall D

# Neutral $\pi^0$ Production from Deuterium : Data

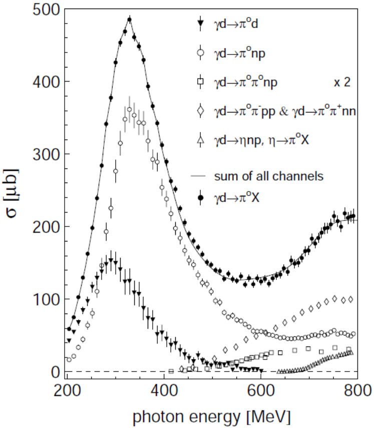


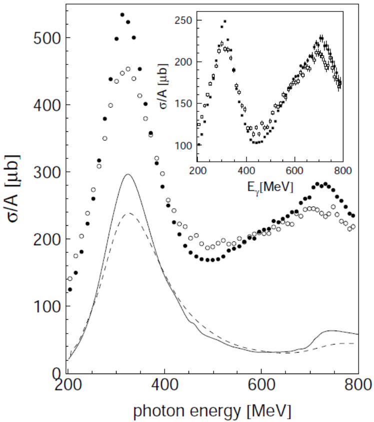


Figure: Left: Neutral pion photoproduction channels and sum of all exclusive channels. Right: Comparison of total photoabsorption (proton : full circle, deuteron open circle ) and neutral meson production (proton : solid curve, deuteron dashed curve ) data. Insert: difference between total photoabsorption and neutral meson production (proton : filled square, deuteron open square) [2]

# Neutral $\pi^0$ Production from Deuterium : Data

- Photoproduction of neutral pions from the deuteron for incident photon energies from 200 *MeV* to 792 *MeV* with the TAPS detector at the Mainz MAMI accelerator.
- Most of the discrepancy between proton and deuteron cross sections comes from the neutral channels
- The difference between total photoabsorption and neutral channels cross section represent the sum of $\pi^{\pm}$,$\pi^+\pi^-$, and $\pi^0\pi^{\pm}$ and should be very similar for proton and deuteron
- Hence cross section ratio of $p(\gamma,\pi^+)n$,$p(\gamma,\pi^0\pi^+)n$,$p(\gamma,\pi^+\pi^-)p$ to $n(\gamma,\pi^-)p$,$n(\gamma,\pi^0\pi^-)p$,$n(\gamma,\pi^+\pi^-)n$ must be close to unity
- Therefore based on this data analysis isospin assumption for deuterium is sufficient to estimate SoLID hadron background

# How to Proceed...

- Preliminary claim : Isospin claim agrees fairly well with data
  - About $10 - 15\%$ agreement with data for total deuterium cross section with isospin symmetry assumption
- GEANT4 Excellent agreement with Proton target (except $\pi^0$) but...
  - Why GEANT4 hadron productions from deuterium deviates from isospin symmetry assumption?
  - Bug in the GEANT4 hadron productions code?
  - Issues with model prediction for nuclear effects like FSI within GEANT4
- Implement deuterium (and $^3He$) properly into Hall D generator : We have a complete hadron background generator for SoLID (more work! and do we really have to do it?)
  - Using SAID and MAID partial-wave analysis models
  - Hall B, MAMI data/fits for deuterium (and $^3He$)
- Once above issues are resolved, SoLID pion asymmetry estimation is also a priority

# Wiser Generator

- Electro and photo production cross-sections derived using Wiser fits are based on SLAC $\gamma\mathrm{N} \rightarrow \mathrm{X}$
  - SLAC bremsstrahlung beam at endpoint energies of 5, 7, 9, 11, 15 and 19 GeV
  - Data were taken for 1 to 8 GeV hadrons with $\mathrm{P_T}$ values from 0.5 GeV to 2.5 GeV
- The fits return the invariant cross section for monochromatic photon beam : $\mathrm{E}' \frac{\mathrm{d}^3\sigma}{\mathrm{dp}'^3}$
- Where $(\mathrm{E}', \mathrm{p}')$ is the hadron momentum and $E_\gamma$ is the incident photon energy
- Wiser fits are available for $\pi^\pm$,$K^\pm$,$P^+$ and $\bar{P}^-$ ($\pi^0$ cross section is the average of $\pi^\pm$ cross sections)

$$E' \frac{d^3\sigma}{dp'^3} = \left( a_1 + \frac{a_2}{\sqrt{s}} \cdot \left(1 - x_R + \frac{a_3^2}{s}\right)^{a_4} \cdot e^{a_5 \cdot M_L} \cdot e^{a_6 \cdot P_T^2/E} \right)$$

where $P_T$ is the transverse momentum of the hadron and $a_i$ are fit parameters.

# Wiser Generator

Photo-Production:

$$\sigma_\mathrm{i} = \int \mathrm{d}\omega \mathrm{N}_\gamma(\omega) \frac{\mathrm{d}\sigma_\mathrm{i}^\gamma(\omega)}{\mathrm{d}\omega}$$

$$\mathrm{N}_\gamma(\omega) = \frac{\mathrm{d}}{\mathrm{X}_0} \frac{\left(\frac{4}{3} - \frac{4\omega}{3\mathrm{E}} + \frac{4\omega^2}{3\mathrm{E}^2}\right)}{\omega}$$

Electro-Production:

$$\sigma_\mathrm{i} = \int \mathrm{d}\omega \mathrm{N}_\mathrm{EPA}(\mathrm{E}_\mathrm{beam}, \omega) \frac{\mathrm{d}\sigma_\mathrm{i}^\gamma(\omega)}{\mathrm{dk}}$$

$$\mathrm{N}_\mathrm{EPA}(\mathrm{E}_\mathrm{beam}, \omega) \simeq \ln\left(\frac{\mathrm{E}_\mathrm{beam}}{\mathrm{m}_\mathrm{e}}\right) \frac{\alpha}{\pi} \frac{1 + (1 - \frac{\omega}{\mathrm{E}_\mathrm{beam}})^2}{\frac{\omega}{\mathrm{E}_\mathrm{beam}}}$$

Where $\omega$ is the photon energy and $\mathrm{E}_\mathrm{beam}$ is the electron beam energy

# Wiser Generator to Get Total Photo-Production Cross Sections

- Wiser fits for electron production cross-sections are based on SLAC $\gamma\mathrm{N} \to \mathrm{X}$
- The fits return the invariant cross section for monochromatic photon beam : $\mathrm{E}' \frac{\mathrm{d}^3\sigma}{\mathrm{dp}'^3}$
- Where $(\mathrm{E}', \mathrm{p}')$ is the hadron momentum and $E_\gamma$ is the incident photon energy
- The total Photo-Production cross section for a monochromatic photon beam for $\mathrm{i}^{\mathrm{th}}$ type interaction,

$$\sigma_{\mathrm{i}}(\mathrm{E}_\gamma) = \int_{\mathrm{phase-space}} \mathrm{E}' \frac{\mathrm{d}^3\sigma}{\mathrm{dp}'^3} \mathrm{dp}'^3$$

- Where subscript i is,

1. $\mathrm{i} = 0, 1 : \pi^\pm$
2. $\mathrm{i} = 2, 3 : K^\pm$
3. $\mathrm{i} = 4, 5 : P^+$ and $\bar{P}^-$

$\pi^0$ cross section is the average of $\pi^\pm$ cross sections

# From Photo-Production to Electro-Production

- Hadron Production can takes place either from real bremsstrahlung photon radiated in the target or from virtual photon interaction approximated by Equivalent Photon Radiator (EPA) approximation
  - Bremsstrahlung contribution is implemented following PDG-2012 [3] and [4]
  - EPA contribution is implemented according to the reference [5]
- Next few slide will summarize the electro-production implementation

# Electro-Production with Equivalent Photon Approximation

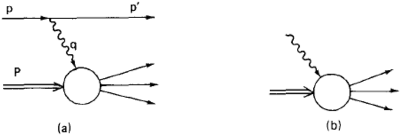


Figure: Electro-Production (a) and Photo-Absorption (b) equivalency [5]

The electro-production cross section for electron energy E using Equivalent Photon Approximation (EPA),

$$d\sigma = \sigma_\gamma(\omega) \cdot dn(\omega)$$

$$dn(\omega) = \int_{q^2_{min}}^{q^2_{max}} dn(\omega, q^2) \qquad = N_{EPA}(\omega)\frac{d\omega}{\omega}$$

where $\sigma_\gamma(\omega)$ is photo-production cross section at photon energy $\omega$ and,

$$N_{EPA}(\omega) = \frac{\alpha}{\pi}\left[\left(1 - \frac{\omega}{E} + \frac{\omega^2}{E^2}\right) ln\frac{q^2_{max}}{q^2_{min}} - \left(1 - \frac{\omega}{2E}\right)^2 ln\frac{(\omega^2+q^2_{max})}{(\omega^2+q^2_{min})} - \frac{m_e^2\omega^2}{E^2 q^2_{min}}\left(1 - \frac{q^2_{min}}{q^2_{max}}\right)\right]$$

# Electro-Production with Radiated Real Photons

The Bremsstrahlung cross section for electron of energy E traveling inside a material [3]

$$\frac{d\sigma}{d\omega} = \frac{A}{X_0 N_A \omega}\left(\frac{4}{3} - \frac{4\omega}{3E} + \frac{4\omega^2}{3E^2}\right)$$

The electro-production cross section due to Bremsstrahlung photons,

$$d\sigma = \sigma_\gamma(\omega) \cdot N_{BREMS}(\omega)\frac{d\omega}{\omega}$$

$$N_{BREMS}(\omega) = \frac{d}{X_0}\left(\frac{4}{3} - \frac{4\omega}{3E} + \frac{4\omega^2}{3E^2}\right)$$

Where $X_0$ is the radiation length and $d = \rho \cdot t$ where $\rho$ is target density and $t$ is target thickness

# Photo-Production with Radiated Real Photons

The Bremsstrahlung cross section for electron of energy E traveling inside a material [3]

$$\frac{d\sigma}{d\omega} = \frac{A}{X_0 N_A \omega}\left(\frac{4}{3} - \frac{4\omega}{3E} + \frac{4\omega^2}{3E^2}\right)$$

The electro-production cross section due to Bremsstrahlung photons,

$$d\sigma = \sigma_\gamma(\omega) \cdot N_\gamma(\omega)\frac{d\omega}{\omega}$$

$$N_\gamma(\omega) = \frac{d}{X_0}\left(\frac{4}{3} - \frac{4\omega}{3E} + \frac{4\omega^2}{3E^2}\right)$$

Where $X_0$ is the radiation length and $d = \rho \cdot t$ where $\rho$ is target density and $t$ is target thickness

# EPA Photon Spectrum

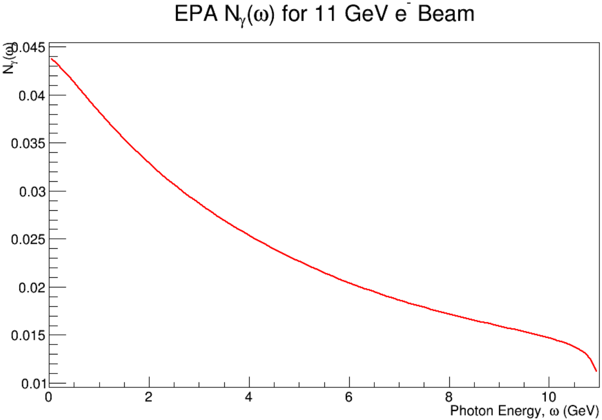


Figure: Photon Spectrum $N_{EPA}(\omega)$

# Bremsstrahlung Photon Spectrum

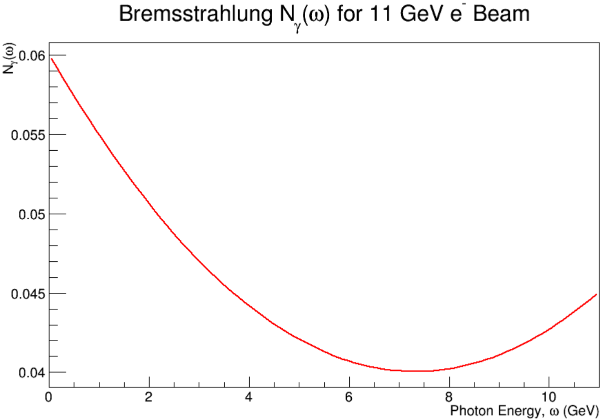


Figure: Photon Spectrum $N_{BREMS}(\omega)$

# Complete Photon Spectrum

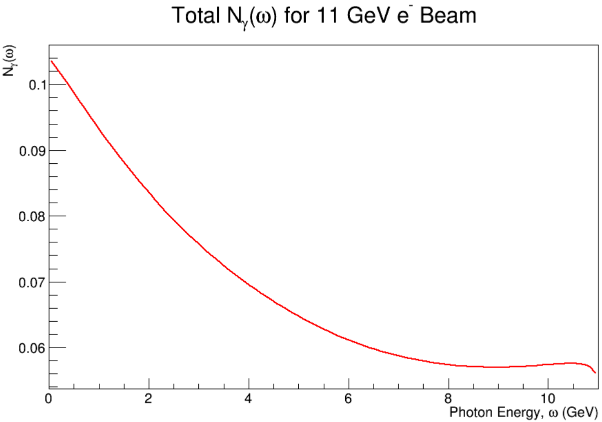


Figure: Photon Spectrum $N_{EPA}(\omega) + N_{BREMS}(\omega)$ for electron incident on a proton target

# Compare Hall D vs. PDG

- Compared total cross sections from Hall D event generator and PDG photo-production cross sections on proton
- For $\gamma$ momentum less than $3\ \mathrm{GeV}$ it uses combination of different models including SAID
- For $\gamma$ momentum greater than $3\ \mathrm{GeV}$ it uses PYTHIA

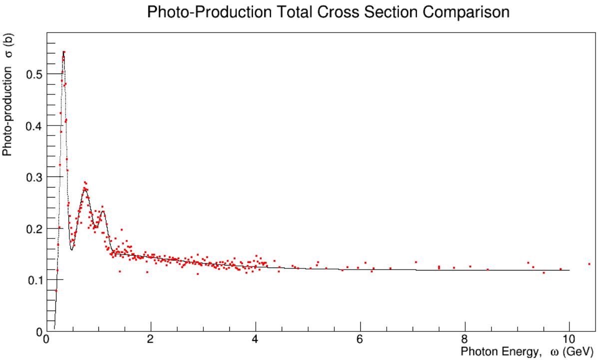


Figure: Black line : Hall D genertor, Red points : PDG

# Hadron Production in GEANT4

- The hadron interactions (say for photo or electro production) in Geant4 are implemented in a two fold method
- Geant4 determines the photonuclear or electronuclear interaction going to take place based on the total cross section
  - For photoproduction cross section, it uses a fit based on models and data.
  - For electroproduction Geant4 uses EPA approximation
- The next step is to simulate the fragmentation of the excited hadronic system in nuclear matter into set of final hadrons
- In earlier versions they used the CHIPS (Chiral Invariant Phase Space) model
- Now it's either Quark Gluon String model + Bertini cascade model (QGSP_BERT) or FTF model which uses a different string model with Bertini cascade model (FTFP_BERT)

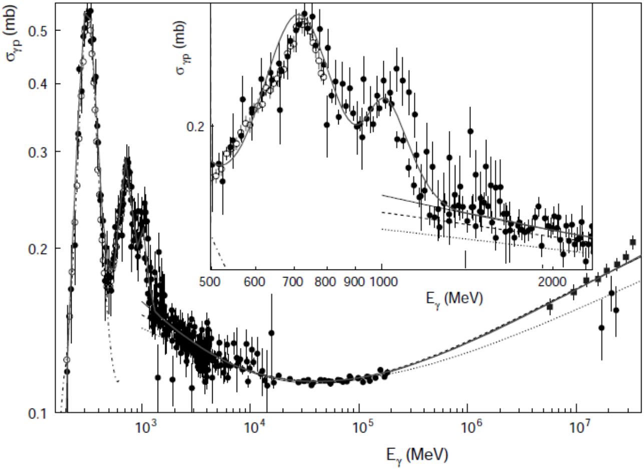


Figure: The thick solid line is the resulting GEANT4 approximation [6]

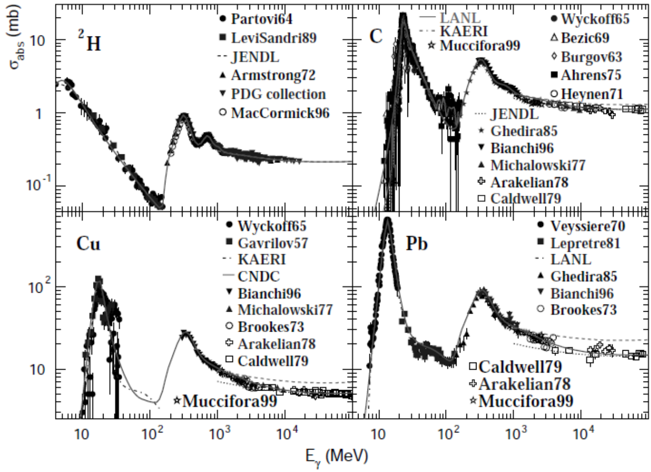


Figure: The thick solid line is the resulting GEANT4 approximation [6]

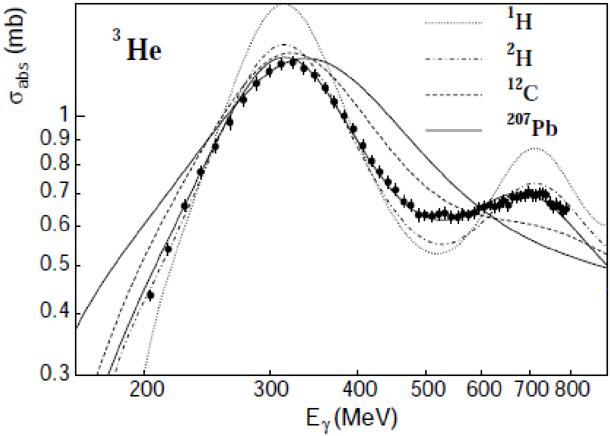


Figure: Thick line the thick solid line is the GEANT4 approximation for 3He. For comparison the approximation curves for 1H (dotted line), 2H (dash-dotted line), C (dashed line), and Pb (thin solid line) are also shown [6]

# Excess $\pi^0$ photo-production on Deuterium in SAMPLE experiment

- Coherent pi0 production $(2H(\gamma, \pi^0)2H)$ in deuterium around the pion threshold
  - Directly from a single nucleon (direct process)
  - From a two-step mechanism where first a charged pion is produced on a one nucleon and then charge exchanges to a $\pi^0$ on a second nucleon $\rightarrow$ rescattering mechanism
- Around the pion threshold rescattering mechanism increases the $\pi^0$ cross section significantly and dominates
  - Then as the energy of the incident photon increases the rescattering terms are still important
- Discussed in the J.C Bergstrom, et. al. paper and they refer to the paper J. H Koch and R. M. Woloshyn, Phys. Rev. C 16, 1968

A. M. Boyarski, D. H. Coward, S. D. Ecklund, B. Richter, D. J. Sherden, R. H. Siemann, and C. K. Sinclair.
Inclusive photoproduction of charged particles in the forward hemisphere.
*Phys. Rev. D*, 14:1733–1771, Oct 1976.

B. Krusche, J. Ahrens, R. Beck, M. Fuchs, S.J. Hall, F. Hrter, J.D. Kellie, V. Metag, M. Rbig-Landau, and H. Strher.
Single and double $\pi^0$ photoproduction from the deuteron.
*The European Physical Journal A - Hadrons and Nuclei*, 6(3):309–324, 1999.

J. Beringer et al.
Review of particle physics.
*Phys. Rev. D*, 86:010001, 2012.

Yung-Su Tsai.
Pair production and bremsstrahlung of charged leptons.
*Rev. Mod. Phys.*, 46:815–851, Oct 1974.

V.M. Budnev, I.F. Ginzburg, G.V. Meledin, and V.G. Serbo.
The two-photon particle production mechanism. physical problems. applications. equivalent photon approximation.
*Physics Reports*, 15(4):181 – 282, 1975.

M.V. Kossov.
Approximation of photonuclear interaction cross-sections.
*Eur. Phys. J. A*, 14(3):377–392, 2002.